Ultrastrong Parametric Coupling between a Superconducting Cavity and a Mechanical Resonator

G. A. Peterson,[1,2] S. Kotler,[1,2] F. Lecocq,[1,2] K. Cicak,[1] X. Y. Jin,[1,2] R. W. Simmonds,[1] J. Aumentado,[1] and J. D. Teufel[1,*]

[1]National Institute of Standards and Technology, 325 Broadway, Boulder, Colorado 80305, USA
[2]Department of Physics, University of Colorado, Boulder, Colorado 80309, USA

(Received 26 June 2019; published 12 December 2019)

We present a new optomechanical device where the motion of a micromechanical membrane couples to a microwave resonance of a three-dimensional superconducting cavity. With this architecture, we realize ultrastrong parametric coupling, where the coupling not only exceeds the dissipation in the system but also rivals the mechanical frequency itself. In this regime, the optomechanical interaction induces a frequency splitting between the hybridized normal modes that reaches 88% of the bare mechanical frequency, limited by the fundamental parametric instability. The coupling also exceeds the mechanical thermal decoherence rate, enabling new applications in ultrafast quantum state transfer and entanglement generation.

DOI: 10.1103/PhysRevLett.123.247701

The physics of coupled oscillators is used to understand a wide array of phenomena, from the microscopic vibrations of atoms and molecules to the interplay of planets and their moons. Coupling strengths can be grouped into different regimes with qualitatively different behavior. In particular, the regimes of weak and strong coupling are distinguished by whether the coupling between two oscillators exceeds their dissipation. In the strong-coupling regime, the eigenfrequencies of the combined system split into normal modes where the energy swaps back and forth between the individual oscillators. For low-loss systems, this energy exchange can be fast compared to the lifetimes of the individual modes, while still remaining slow compared to their periods. The strong-coupling regime has become an essential tool in engineered quantum systems because it can allow the subsystems to exchange their quantum information before it is lost due to decoherence [1]. As quantum devices continue to be engineered with larger coupling rates, a new regime known as ultrastrong coupling has become increasingly relevant. This regime occurs once the coupling becomes so large as to rival a bare resonance frequency, resulting in new quantum effects, including multimode entanglement and nontrivial ground states. While ultrastrong coupling has been demonstrated in a handful of quantum systems, including superconducting qubits and semiconducting quantum wells, a complete understanding of its physics and applications continues to emerge as a variety of new physical systems encounter this regime [2,3]. Here, we extend the experimental study of ultrastrong coupling to parametrically coupled quantum harmonic oscillators in a cavity optomechanical system.

Cavity optomechanics is an area of engineered quantum systems in which a mechanical resonator and an electromagnetic mode form a coupled-oscillator system [4]. Although the intrinsic coupling between single photons and phonons is typically small, cavity optomechanical systems allow an enhancement of the coupling proportional to the amplitude of a coherent cavity drive. This parametric enhancement has enabled demonstrations of strong coupling both at ambient temperatures [5,6] and in cryogenic quantum-coherent regimes [7–10]. In practice, as the intensity of the coherent drive becomes large, it can induce other undesirable effects, including heating and cavity nonlinearity, limiting the final parametric coupling. Operating deep within the quantum-coherent ultrastrong-coupling regime therefore requires a dramatic increase in either the single-photon optomechanical coupling or the cavity's power handling capability. Specifically, in the microwave domain, one prominent optomechanical platform is a lumped element superconducting circuit formed from a mechanically compliant capacitor shunted by a thin-film inductor. While this architecture has enabled strong coupling [7], ground-state cooling [11], and entanglement [12], the coupling has remained well below the onset of ultrastrong-coupling effects, limited by unwanted nonlinearity of the superconducting inductor due to its kinetic inductance [13,14].

In this Letter, we introduce a new optomechanical architecture that mitigates the nonideality of previous designs, allowing us to reach ultrastrong coupling and the fundamental stability limit of the optomechanical interaction [15]. Our device consists of a microfabricated vacuum-gap capacitor embedded in a three-dimensional superconducting microwave cavity, analogous to recent work in circuit quantum electrodynamics [16] and similar to other optomechanical demonstrations [9,17–19]. Our device takes advantage of the superior power handling of bulk cavity resonators compared to thin-film inductors owing to their larger surface areas and correspondingly smaller current

densities [20]. In general, the drawback of using a cavity resonator is a larger parasitic capacitance that would dilute the optomechanical coupling. Crucially, through careful microwave design and simulation, we maintain the relatively large single-photon coupling of lumped element circuits [7]. As a result, we achieve ultrastrong parametric coupling by applying microwave drives with 100 times larger power, ultimately limited by the instability inherent in the optomechanical Hamiltonian. Because of the low temperature of operation, the quantum decoherence rates are kept sufficiently small to enable new regimes of entanglement [15,21], nonlinear quantum optomechanics [22], and ultrafast quantum state transfer [12,23,24].

In a cavity optomechanical system, the frequency ω_c of an electromagnetic resonance depends on the position $\hat{x}$ of a harmonic oscillator [4]. The interaction Hamiltonian is $\hat{H}_{\rm int} = \hbar g_0 \hat{n}\,\hat{x}/x_{\rm zp}$, where g_0 is the single-photon coupling, $\hat{n}$ is the number operator for microwave photons, and $\hbar$ is the reduced Planck constant. $x_{\rm zp} = \sqrt{\hbar/2m\Omega}$ is the mechanical zero-point fluctuation amplitude, where m and Ω are the effective mass and the resonance frequency of the mechanical mode. Dissipation is characterized by damping rates κ for the electrical mode and Γ for the mechanical mode, with $\Gamma \ll \kappa$. Even if g_0 is small, the coupling can be parametrically enhanced by driving the electrical mode to a coherent state of mean photon number n_d at frequency ω_d. Defining $\hat{a}$ as the annihilation operator for fluctuations around the driven state, we can approximate the interaction Hamiltonian as $\hat{H}_{\rm int} = \hbar g(\hat{a} + \hat{a}^\dagger)\hat{x}/x_{\rm zp}$, where $g = g_0\sqrt{n_d}$ is the parametrically enhanced coupling, leading to a set of linear equations of motion for $\hat{a}(t)$ and $\hat{x}(t)$. Just as two passively coupled oscillators interact most strongly when resonant with each other, parametric coupling creates an effective resonance condition when the system is driven at the difference frequency ($\Delta \equiv \omega_d - \omega_c = -\Omega$) in the resolved sideband regime ($\kappa \ll \Omega$). These conditions optimize the coherent exchange of energy between the mechanical and electromagnetic modes.

As the driven coupling g is increased from its single-photon value, we encounter several distinct regimes of coupling. When the cooperativity $C = 4g^2/\kappa\Gamma$ reaches one, the optical damping of the mechanical mode begins to dominate over its intrinsic dissipation. As g increases further, the effective mechanical linewidth increases until it reaches the cavity dissipation when $g = \kappa/4$. Above this threshold, the system enters the strong-coupling regime, where the cavity and mechanical modes hybridize, with the mechanical resonance frequency splitting into two solutions, which for $g \ll \Omega$ are given by

$$\Omega_\pm \simeq \Omega \pm \sqrt{g^2 - \kappa^2/16}. \tag{1}$$

This leads to the splitting $\Omega_s = \Omega_+ - \Omega_- \simeq 2g$ when the coupling overwhelms the cavity dissipation. In this regime of strong coupling, the two resonators exchange energy at a rate Ω_s, faster than any dissipation in the system.

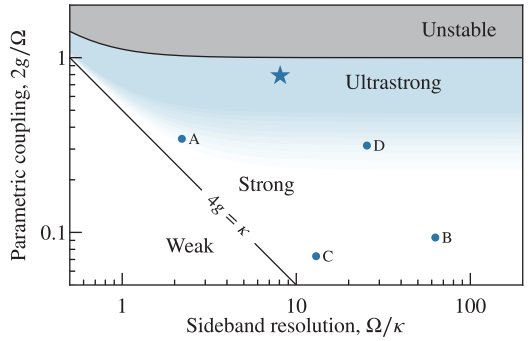

FIG. 1. Parameter space diagram showing four regimes of parametric optomechanical coupling g as a function of cavity dissipation κ and mechanical frequency Ω. For a parametric drive at $\Delta = -\Omega$, strong coupling coincides with the normal-mode splitting condition $\kappa < 4g$. Ultrastrong coupling arises when g further increases to a significant fraction of Ω until reaching the limit for stability at $2g = \sqrt{\Omega^2 + \kappa^2/4}$. Labeled points denote previous optomechanical experiments in the strong-coupling regime: (A) optical Fabry-Pérot cavity [5], (B) lumped element microwave circuit [7], (C) toroidal optical microcavity [8], and (D) microwave loop-gap cavity [9]. The star indicates the highest coupling achieved in this Letter.

As the splitting Ω_s approaches the mechanical frequency Ω, however, terms of order g/Ω cannot be ignored, requiring the use of the exact eigenfrequency spectrum (see Supplemental Material [25])

$$\Omega_\pm = {\rm Re}\sqrt{\Omega^2 - \frac{\kappa^2}{16} \pm 2\Omega\sqrt{g^2 - \frac{\kappa^2}{16}}}. \tag{2}$$

The discrepancy between (1) and (2) is a measurable metric to distinguish strong and ultrastrong parametric coupling. In the resolved sideband ultrastrong-coupling regime ($\kappa \ll 2g < \Omega$), Eq. (2) becomes $\Omega_\pm \simeq \Omega\sqrt{1 \pm 2g/\Omega}$, showing that the splitting exceeds $2g$. When the coupling reaches $\Omega/2$ with a splitting of $\Omega_s = \sqrt{2}\Omega$, the lower eigenfrequency goes to zero, and the effective mode dissipation becomes negative [25]; here, the system becomes parametrically unstable, with mode amplitudes exponentially growing in time.

These regimes are shown in Fig. 1 as a function of parametric coupling and sideband resolution Ω/κ. The shaded region of ultrastrong coupling corresponds to $\Omega/5 < \Omega_s$, roughly where terms of order g/Ω become relevant while still satisfying the condition for strong coupling. As Ω_s characterizes the energy exchange rate, the instability sets a fundamental limit for both optomechanical coupling and coherent transfer of information between the resonators in the steady state.

For quantum applications, the coupling should be compared not only to dissipation but also to decoherence

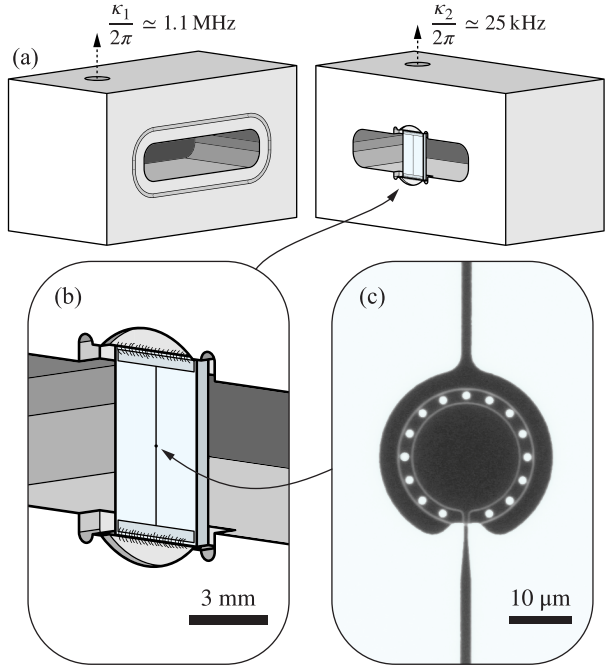

FIG. 2. Device schematic. (a) A cavity, milled from two aluminum blocks, supports a microwave resonance near 12 GHz. Microwave signals couple in and out of the cavity through two asymmetrically coupled ports. (b) An aluminum mechanically compliant capacitor patterned on a sapphire substrate is galvanically connected to the cavity walls through superconducting wire bonds, loading the fundamental cavity resonance frequency down to 6.5 GHz. (c) A micrograph image shows the capacitor, which has a fundamental mechanical resonance at 9.7 MHz and a vacuum gap of approximately 30 nm.

in the system. In particular, the mechanical thermal decoherence $n_{\mathrm{th}}\Gamma$ can be much larger than the intrinsic dissipation Γ, where n_{th} is the occupancy of the mechanical thermal environment. Ideally, the quantum cooperativity $C_q = 4g^2/\kappa n_{\mathrm{th}}\Gamma$ exceeds one before the onset of strong coupling, ensuring that the hybridized system is quantum coherent. In the following, we present an optomechanical device that achieves the hierarchy of rates desired for quantum-coherent ultrastrong coupling: $n_{\mathrm{th}}\Gamma \ll \kappa/2 \ll 2g \lesssim \Omega \ll \omega_c$.

Our device is shown in Fig. 2. A microwave cavity resonator with inner dimensions $19 \times 4 \times 17$ mm milled from bulk aluminum defines the electrical resonance of the system [26]. We focus on the fundamental TE_{101} microwave mode, whose electric field is maximal at the center of the cavity, where we place a sapphire chip containing a microfabricated 20 μm-diameter aluminum vacuum-gap capacitor [23]. The suspended top plate of the capacitor forms the mechanical resonator of the system. Reducing the parasitic capacitance of the cavity and thereby maximizing the optomechanical coupling requires a galvanic connection between the microfabricated capacitor and the cavity walls. To achieve this, we use aluminum bond wires to connect the cavity faces to lithographically patterned pads, which then connect to the capacitor through thin-film aluminum wires.

The vacuum-gap capacitor and sapphire substrate load the cavity resonance, pulling its frequency from around 12 GHz down to $\omega_c/2\pi \approx 6.506$ GHz. Two cavity ports with adjustable coupling pins allow signals to couple in and out to coaxial cables. We adjust the length of the pins at room temperature so the two ports contribute asymmetrically to the total dissipation $\kappa = \kappa_1 + \kappa_2 + \kappa_i$, where $\kappa_1/2\pi \approx 1.1$ MHz and $\kappa_2/2\pi \approx 25$ kHz are the port coupling rates. The internal dissipation rate $\kappa_i/2\pi$ of the cavity mode ranges from $\sim$30 to $\sim$140 kHz depending on the circulating power [27]. We place the device in a cryostat with a base temperature of 16 mK and probe the system with microwave signals applied near the cavity resonance frequency. Our setup allows us to measure all four elements of the scattering matrix for a broad range of parametric coupling parameters. With a weak cavity drive, we characterize the fundamental vibrational mode of the capacitor plate by its resonance frequency $\Omega/2\pi \approx 9.696$ MHz and its intrinsic damping rate $\Gamma/2\pi = (31 \pm 1)$ Hz, where the uncertainty represents the standard error of the mean. By varying the cryostat temperature and measuring mechanical thermal noise, we determine the single-photon optomechanical coupling rate $g_0/2\pi = (167 \pm 2)$ Hz [11]. At base temperature, the mechanical mode equilibrates to (35 ± 3) mK, corresponding to a thermal phonon occupancy $n_{\mathrm{th}} = 76 \pm 6$.

To probe the response of the coupled system, we measure the transmission of a weak microwave probe through the cavity in the presence of a parametric drive [7,28,29]. In Fig. 3, we plot the transmission of the probe for a range of drive powers applied below the cavity resonance, with the drive frequency indicated as a red vertical line. We coherently cancel the drive after it leaves the cavity, allowing us to measure the transmission of a weak probe without saturating our microwave measurement (see Supplemental Material [25]). We adjust the drive frequency as we increase drive power to maintain the condition $\Delta = -\Omega$ in the presence of two dominant nonlinear effects. Namely, we measure the pure optomechanical Kerr shift, $-2g_0^2/\Omega = (-5.8 \pm 0.1)$ mHz/photon, and we attribute the remaining shift to the residual nonlinear kinetic inductance of the superconducting film [13,14], approximately -4 mHz/photon, at our highest powers, roughly an order of magnitude smaller than in previous lumped element designs.

At low drive power [Fig. 3(a)], we measure the bare cavity resonance. As the drive power increases [Fig. 3(b)], optomechanical interference appears in the cavity response over a bandwidth $\sim 4g^2/\kappa$. At large enough power [Fig. 3(c)], the damped mechanical width reaches $\kappa/2$, after which the response splits into normal modes, marking the strong-coupling regime. Additionally, we begin to resolve the next four vibrational modes of the membrane [sharp features in Figs. 3(d) and 3(e)], which couple weakly to the cavity mode.

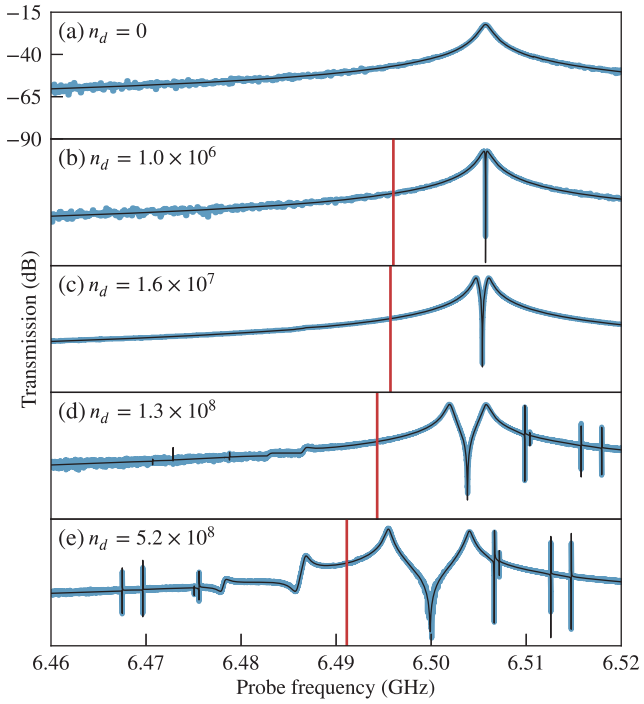

FIG. 3. Measured and calibrated cavity transmission from port 1 to port 2 for varied drive strengths n_d from weak coupling [(a), (b)] through strong coupling [(c),(d)] and up to ultrastrong coupling (e). The data (blue) are fit to theory (black) containing the first five mechanical modes. The vertical red line indicates the frequency of the applied microwave drive, adjusted to maintain $\Delta = -\Omega$. The structure below the drive frequency at the highest powers directly shows the importance of counterrotating terms in the ultrastrong-coupling regime.

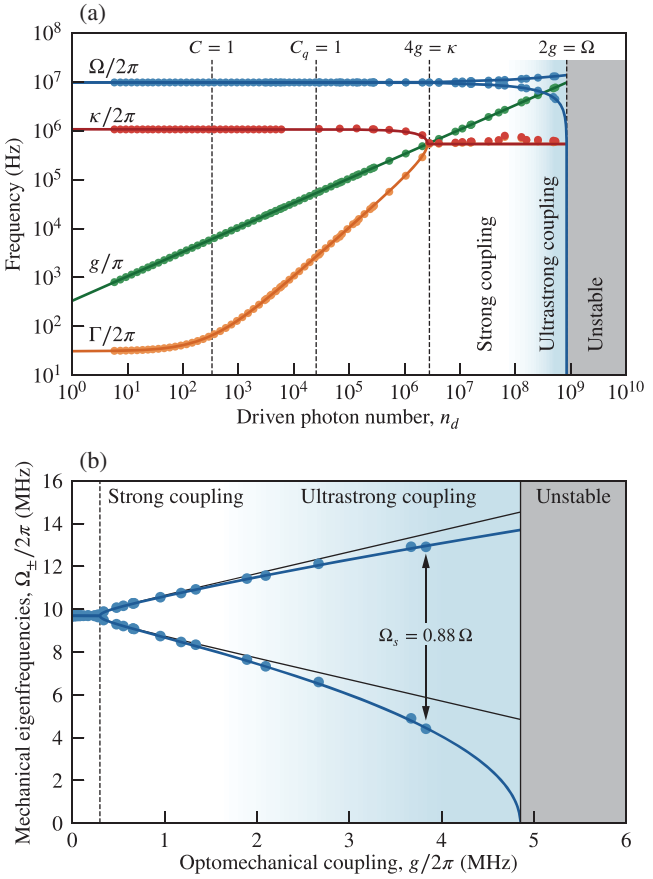

FIG. 4. (a) Measured system rates as a function of drive strength. In the weak-coupling regime, the optical damping first exceeds the mechanical dissipation ($C = 1$) and then exceeds the thermal decoherence ($C_q = 1$). Once $2g$ reaches $\kappa/2$, the eigenmodes split, indicating the onset of strong coupling. Eventually, ultrastrong-coupling corrections become important before the system approaches a parametric instability at $2g = \Omega$. (b) Mechanical eigenfrequencies as a function of the optomechanical coupling. In the ultrastrong-coupling regime, the splitting $\Omega_s = \Omega_+ - \Omega_-$ exceeds the linear strong-coupling approximation $\Omega_s \simeq 2g$ (black), reaching a maximal value $\Omega_s \approx 0.88\Omega$.

At the highest power [Fig. 3(e)], the response acquires several features indicative of ultrastrong coupling. In addition to the splitting of the fundamental resonance becoming of order Ω, the dynamics below the drive frequency become significant and easily observable. Lastly, the transmission at the drive frequency begins to increase, signifying a nonlinear relationship between input power and driven photon number in the cavity.

We fit the complex data to multimode optomechanical theory (see Supplemental Material [25]), shown as a black line plotted over the data. The quantitative agreement between data and theory allows us to extract all relevant system parameters as a function of drive power. These parameters are shown in Fig. 4(a) from weak to ultrastrong parametric coupling. For few drive photons ($n_d \lesssim 10^2$), the bare mode properties are measured. As the drive power increases within the regime of weak coupling ($n_d \lesssim 10^6$), the mechanical mode is damped and cooled, passing through $C = 1$ and entering the quantum regime $C_q > 1$, where the occupancy is reduced below one quantum. Normal-mode splitting occurs at $n_d \approx 3 \times 10^6$, where $4g = \kappa$, marking the beginning of strong coupling. Above $n_d \approx 2 \times 10^8$, the splitting starts to deviate from $2g$ as the coupling becomes ultrastrong. The threshold for parametric oscillation occurs at $n_d \approx 8.4 \times 10^8$, above which no steady-state solution exists. We measure well into the regime where $\Omega_- < 2g < \Omega_s$; that is, the energy swapping rate exceeds $2g$ as well as the lower eigenfrequency itself.

In Fig. 4(b), the measured mechanical eigenfrequencies are plotted vs the optomechanical coupling. The black line shows the strong-coupling approximation (1), while the full solution (2) is shown in blue. The discrepancy between the two indicates ultrastrong coupling. At the highest power, the splitting between the two modes exceeds the frequency of the lower mode, reaching 88% of the bare mechanical frequency.

Our measurements of the driven cavity response allow us to reconstruct the mechanical susceptibility $\chi_m(\omega)$,

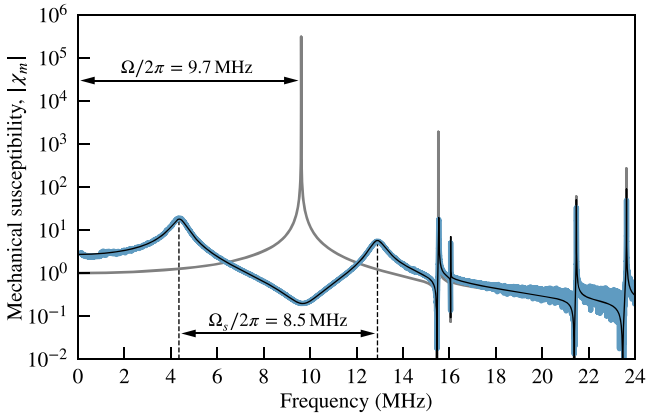

FIG. 5. Mechanical susceptibility inferred from microwave measurements at our highest drive power (blue) with fit line (black) compared with the bare susceptibility (gray). The susceptibility in the ultrastrong-coupling regime shows asymmetry at the two eigenfrequencies as well as a marked increase in its value at zero frequency, in agreement with the full theory.

including the first four higher-order vibrational modes (Fig. 5). The original fundamental mode of linewidth Γ splits into two broad peaks with approximate widths $\kappa/2$, each representing a normal mode of the joint cavity–mechanical system. At our highest cooperativity of $C \approx 1.6 \times 10^6$, we achieve a maximal splitting of $\Omega_s/2\pi \approx 8.5$ MHz. Here, the mechanical state is exchanged with the cavity in a characteristic time $\pi/\Omega_s \approx 60$ ns, faster than the mechanical oscillation period $2\pi/\Omega \approx 100$ ns.

In conclusion, we have introduced a novel optomechanical architecture and experimentally characterized it in the ultrastrong-coupling regime. Looking forward, ultrastrongly coupled linear modes are predicted to have interesting ground-state properties [30–33]. In this regime, quantum correlations induce squeezing and mechanical-cavity entanglement [21]. Studying the noise properties here would allow us to observe these effects for the first time and assess how these correlations could be exploited for quantum-enhanced sensing [34–36]. Furthermore, while the instability precludes steady-state measurements when the swapping rate exceeds the mechanical frequency, pulsed measurements would allow characterization beyond this limit into the deep strong-coupling regime [2,3], enabling new regimes of quantum state transfer [24,37], entanglement [12], topologically protected operations [38], and projective measurements [39]. Finally, theoretical proposals have suggested using ultrastrong coupling to enhance the weak nonlinear terms of the optomechanical Hamiltonian [22] allowing for nonlinear quantum optomechanics.

G. A. P. acknowledges support from the National Physical Science Consortium. Contributions to this article by workers at NIST, an agency of the U.S. Government, are not not subject to U.S. copyright.

*Corresponding author.
john.teufel@nist.gov

[1] H. Mabuchi and A. C. Doherty, Cavity quantum electrodynamics: Coherence in context, Science **298**, 1372 (2002).
[2] A. F. Kockum, A. Miranowicz, S. De Liberato, S. Savasta, and F. Nori, Ultrastrong coupling between light and matter, Nat. Rev. Phys. **1**, 19 (2019).
[3] P. Forn-Díaz, L. Lamata, E. Rico, J. Kono, and E. Solano, Ultrastrong coupling regimes of light-matter interaction, Rev. Mod. Phys. **91**, 025005 (2019).
[4] M. Aspelmeyer, T. J. Kippenberg, and F. Marquardt, Cavity optomechanics, Rev. Mod. Phys. **86**, 1391 (2014).
[5] S. Gröblacher, K. Hammerer, M. R. Vanner, and M. Aspelmeyer, Observation of strong coupling between a micromechanical resonator and an optical cavity field, Nature (London) **460**, 724 (2009).
[6] G. Enzian, M. Szczykulska, J. Silver, L. Del Bino, S. Zhang, I. A. Walmsley, P. Del'Haye, and M. R. Vanner, Observation of Brillouin optomechanical strong coupling with an 11 GHz mechanical mode, Optica **6**, 7 (2019).
[7] J. D. Teufel, D. Li, M. S. Allman, K. Cicak, A. J. Sirois, J. D. Whittaker, and R. W. Simmonds, Circuit cavity electromechanics in the strong-coupling regime, Nature (London) **471**, 204 (2011).
[8] E. Verhagen, S. Deléglise, S. Weis, A. Schliesser, and T. J. Kippenberg, Quantum-coherent coupling of a mechanical oscillator to an optical cavity mode, Nature (London) **482**, 63 (2012).
[9] A. Noguchi, R. Yamazaki, M. Ataka, H. Fujita, Y. Tabuchi, T. Ishikawa, K. Usami, and Y. Nakamura, Ground state cooling of a quantum electromechanical system with a silicon nitride membrane in a 3D loop-gap cavity, New J. Phys. **18**, 103036 (2016).
[10] P. Kharel, Y. Chu, E. A. Kittlaus, N. T. Otterstrom, S. Gertler, and P. T. Rakich, Multimode strong coupling in cavity optomechanics, arXiv:1812.06202.
[11] J. D. Teufel, T. Donner, D. Li, J. W. Harlow, M. S. Allman, K. Cicak, A. J. Sirois, J. D. Whittaker, K. W. Lehnert, and R. W. Simmonds, Sideband cooling of micromechanical motion to the quantum ground state, Nature (London) **475**, 359 (2011).
[12] T. A. Palomaki, J. D. Teufel, R. W. Simmonds, and K. W. Lehnert, Entangling mechanical motion with microwave fields, Science **342**, 710 (2013).
[13] M. A. Golosovsky, H. J. Snortland, and M. R. Beasley, Nonlinear microwave properties of superconducting nb microstrip resonators, Phys. Rev. B **51**, 6462 (1995).
[14] J. Zmuidzinas, Superconducting microresonators: Physics and applications, Annu. Rev. Condens. Matter Phys. **3**, 169 (2012).
[15] S. Aldana, C. Bruder, and A. Nunnenkamp, Equivalence between an optomechanical system and a Kerr medium, Phys. Rev. A **88**, 043826 (2013).
[16] H. Paik, D. I. Schuster, L. S. Bishop, G. Kirchmair, G. Catelani, A. P. Sears, B. R. Johnson, M. J. Reagor, L. Frunzio, L. I. Glazman, S. M. Girvin, M. H. Devoret, and R. J. Schoelkopf, Observation of High Coherence in Josephson Junction Qubits Measured in a Three-Dimensional Circuit QED Architecture, Phys. Rev. Lett. **107**, 240501 (2011).

[17] M. E. Tobar and D. G. Blair, Parametric transducers for resonant bar gravitational wave antennae, J. Phys. D **26**, 2276 (1993).

[18] M. Yuan, V. Singh, Y. M. Blanter, and G. A. Steele, Large cooperativity and microkelvin cooling with a three-dimensional optomechanical cavity, Nat. Commun. **6**, 8491 (2015).

[19] B. Gunupudi, S. R. Das, R. Navarathna, S. K. Sahu, S. Majumder, and V. Singh, An Optomechanical Platform with a Three-Dimensional Waveguide Cavity, Phys. Rev. Applied **11**, 024067 (2019).

[20] M. Reagor, H. Paik, G. Catelani, L. Sun, C. Axline, E. Holland, I. M. Pop, N. A. Masluk, T. Brecht, L. Frunzio, M. H. Devoret, L. Glazman, and R. J. Schoelkopf, Reaching 10 ms single photon lifetimes for superconducting aluminum cavities, Appl. Phys. Lett. **102**, 192604 (2013).

[21] S. G. Hofer and K. Hammerer, Entanglement-enhanced time-continuous quantum control in optomechanics, Phys. Rev. A **91**, 033822 (2015).

[22] M.-A. Lemonde, N. Didier, and A. A. Clerk, Nonlinear Interaction Effects in a Strongly Driven Optomechanical Cavity, Phys. Rev. Lett. **111**, 053602 (2013).

[23] F. Lecocq, J. D. Teufel, J. Aumentado, and R. W. Simmonds, Resolving the vacuum fluctuations of an optomechanical system using an artificial atom, Nat. Phys. **11**, 635 (2015), see Supplemental Material.

[24] A. P. Reed, K. H. Mayer, J. D. Teufel, L. D. Burkhart, W. Pfaff, M. Reagor, L. Sletten, X. Ma, R. J. Schoelkopf, E. Knill, and K. W. Lehnert, Faithful conversion of propagating quantum information to mechanical motion, Nat. Phys. **13**, 1163 (2017).

[25] See Supplemental Information at http://link.aps.org/supplemental/10.1103/PhysRevLett.123.247701 for the theory of ultrastrong optomechanical coupling and additional experimental information.

[26] X. Y. Jin, A. Kamal, A. P. Sears, T. Gudmundsen, D. Hover, J. Miloshi, R. Slattery, F. Yan, J. Yoder, T. P. Orlando, S. Gustavsson, and W. D. Oliver, Thermal and Residual Excited-State Population in a 3D Transmon Qubit, Phys. Rev. Lett. **114**, 240501 (2015).

[27] J. M. Martinis, K. B. Cooper, R. McDermott, M. Steffen, M. Ansmann, K. D. Osborn, K. Cicak, S. Oh, D. P. Pappas, R. W. Simmonds, and C. C. Yu, Decoherence in Josephson Qubits from Dielectric Loss, Phys. Rev. Lett. **95**, 210503 (2005).

[28] S. Weis, R. Rivière, S. Deléglise, E. Gavartin, O. Arcizet, A. Schliesser, and T. J. Kippenberg, Optomechanically induced transparency, Science **330**, 1520 (2010).

[29] A. H. Safavi-Naeini, T. P. Mayer Alegre, J. Chan, M. Eichenfield, M. Winger, Q. Lin, J. T. Hill, D. E. Chang, and O. Painter, Electromagnetically induced transparency and slow light with optomechanics, Nature (London) **472**, 69 (2011).

[30] C. Ciuti, G. Bastard, and I. Carusotto, Quantum vacuum properties of the intersubband cavity polariton field, Phys. Rev. B **72**, 115303 (2005).

[31] C. Ciuti and I. Carusotto, Input-output theory of cavities in the ultrastrong coupling regime: The case of time-independent cavity parameters, Phys. Rev. A **74**, 033811 (2006).

[32] S. Fedortchenko, S. Felicetti, D. Marković, S. Jezouin, A. Keller, T. Coudreau, B. Huard, and P. Milman, Quantum simulation of ultrastrongly coupled bosonic modes using superconducting circuits, Phys. Rev. A **95**, 042313 (2017).

[33] D. Marković, S. Jezouin, Q. Ficheux, S. Fedortchenko, S. Felicetti, T. Coudreau, P. Milman, Z. Leghtas, and B. Huard, Demonstration of an Effective Ultrastrong Coupling between Two Oscillators, Phys. Rev. Lett. **121**, 040505 (2018).

[34] R. Schnabel, N. Mavalvala, D. E. McClelland, and P. K. Lam, Quantum metrology for gravitational wave astronomy, Nat. Commun. **1**, 121 (2010).

[35] N. S. Kampel, R. W. Peterson, R. Fischer, P.-L. Yu, K. Cicak, R. W. Simmonds, K. W. Lehnert, and C. A. Regal, Improving Broadband Displacement Detection with Quantum Correlations, Phys. Rev. X **7**, 021008 (2017).

[36] D. Mason, J. Chen, M. Rossi, Y. Tsaturyan, and A. Schliesser, Continuous force and displacement measurement below the standard quantum limit, Nat. Phys. **15**, 745 (2019).

[37] T. A. Palomaki, J. W. Harlow, J. D. Teufel, R. W. Simmonds, and K. W. Lehnert, Coherent state transfer between itinerant microwave fields and a mechanical oscillator, Nature (London) **495**, 210 (2013).

[38] H. Xu, D. Mason, L. Jiang, and J. G. E. Harris, Topological energy transfer in an optomechanical system with exceptional points, Nature (London) **537**, 80 (2016).

[39] M. R. Vanner, I. Pikovski, G. D. Cole, M. S. Kim, Č. Brukner, K. Hammerer, G. J. Milburn, and M. Aspelmeyer, Pulsed quantum optomechanics, Proc. Natl. Acad. Sci. U.S.A. **108**, 16182 (2011).